

Two-Fluid and PIC-Fluid Code Comparison of the Plasma Plume in a Magnetic Nozzle

J. Navarro* and M. Merino† and E. Ahedo‡

Universidad Politécnica de Madrid, Madrid 28040 Spain

The HPMN hybrid (PIC/fluid) code is characterized and validated against the DIMAGNO two-fluid, collisionless code of the plasma flow in a magnetic nozzle. A globally current-free, fully-ionized plasma generated by a helicon source is injected at the magnetic nozzle throat of each code and simulated. Comparison of the plasma properties of each solution highlights the differences and similarities between both codes. Results on main plasma magnitudes agree well, supporting the validity and accuracy of HPMN and suggesting points of further improvement.

I. Introduction

Magnetic nozzles (MN) are envisaged as a promising acceleration system for advanced plasma thrusters. By using an axisymmetric, divergent applied magnetic field, the hot plasma of these engines can be efficiently channeled and expanded into vacuum to produce thrust in an equivalent way to a solid de Laval nozzle. The central advantages of MN over their solid counterparts are the strong reduction of plasma losses and wall damage thanks to magnetic confinement, and the possibility to control thrust and specific impulse in flight by modifying the geometry and intensity of the applied field, which allows to adapt to different mission profiles. Examples of electric thrusters using of MN are: the Helicon thruster,¹⁻⁴ the applied-field MPD thruster^{5,6} and the VASIMIR.⁷ Once accelerated, the plasma needs to free itself from the imposed magnetic field to form a directed axial beam, a phenomenon known as detachment.

A good understanding of plasma physics in the MN is central for the development of a successful and efficient thruster that can compete with the current array of highly optimized electric propulsion systems, or extend the current performance envelope. In this regard, numerical simulations are of paramount importance to attain this understanding and complement experiments, since they can provide the necessary insight in the mechanisms for plasma acceleration and detachment.

In the last years, we have studied the physics of the MN with DIMAGNO,⁸⁻¹⁰ a two fluid, two dimensional code of a totally ionized, quasineutral, collisionless plasma. DIMAGNO code reproduces the fundamental physics of the MN, including fluxes of ions and electrons, electric potential, electric currents and induced magnetic fields. It achieves high computational speed and accuracy thanks to the Method of Characteristics (MoC) used in the integration of the supersonic flow. This code has permitted the analysis of the acceleration mechanisms in the nozzle, the radial rarefaction of the expansion, the generation and transmission of thrust, and the parametric investigation of propulsive performances.⁸ Additionally, an initial study of the detachment problem in a hot plasma has been carried out, where DIMAGNO showed that plasma induced magnetic field, resistivity, and azimuthal electron inertia cause radially-outwards detachment.⁹

In spite of its success and adequacy for the study of the fundamental physics of a MN, the approach followed in DIMAGNO is constrained by the assumption of a collisionless plasma and the inherent characteristics of a fluid model, precluding the analysis of interesting phenomena such as resistive diffusion in the plume. To overcome this and other limitations, a 2D hybrid particle/fluid, quasineutral code called HPMN after 'hybrid particle magnetic nozzle' has been developed at EP2.¹¹ This code nourishes on the large experience and confidence acquired on the well-tested HPHall2 code used in our group,¹² originally conceived for

*PhD student, Equipo de Propulsión Espacial y Plasmas (EP2), web.fmetsia.upm.es/ep2), student AIAA member (jaume.navarro@upm.es).

†PhD student, EP2, student AIAA member (mario.merino@upm.es).

‡Professor, EP2, senior AIAA member (eduardo.ahedo@upm.es).

the simulation of Hall effect thrusters. In HPMN, heavy species are simulated with the particle-in-cell (PIC) methodology, while fully-magnetized electrons are modeled as a magnetized fluid. Collisions are treated with Monte Carlo (MC) methods. This hybrid approach means a convenient trade-off between complexity and detail, and allows to recover physical aspects unattainable with a fully fluid model, such as the ion energy distribution function (EDF). However, some accuracy and the “cleanness” which characterize fluid models such as DIMAGNO are unavoidably sacrificed. One the advantages of the HPMN code is that it takes into account electron collision effects, and allows exploring the gentle diffusive transition between the dense jet and the near-vacuum region, whereas DIMAGNO necessarily employs a sharp plasma-vacuum edge.

The goal of this paper is, first of all, to carry out the validation of the HPMN code. Validation of this newer code needs to be performed based on previous knowledge of MNs. To this end, identical plasma flows are simulated with DIMAGNO and HPMN, and we compare and cross-validate the results. The calculated plasma profile at the exit of a helicon source will be employed in both simulations. Comparisons are made in terms of plasma density distribution, ion current density flows, induced azimuthal currents, and thrust gain. From this analysis, we reach conclusions about the suitability of each code to simulate the different physics present in a MN. Our second objective is the investigation and characterization of the new physical phenomena present in HPMN that were unavailable in DIMAGNO. Our focus here is on the diffusion due to collisions.

The paper is organized as follows. First, a short summary of the fluid model of DIMAGNO and the hybrid model of HPMN is provided in sections II and III, respectively. Then, in section IV, the upstream plasma provided by a helicon source is characterized. This knowledge provides the initial flow conditions for the simulations of DIMAGNO and HPMN. The comparison of results and the main discussion is carried out in section V. Finally, conclusions and planned future developments are gathered in section VI.

II. Fluid model (DIMAGNO)

Summarily, the fluid model of DIMAGNO describes the axisymmetric, steady-state flow of a totally-ionized, quasineutral, collisionless, supersonic plasma in the divergent magnetic field \mathbf{B} . Electrons are modeled as a hot, isotropic species of constant temperature T_e , while ions are modeled as a cold one with mass m_i . A detailed account of the derivation of the model, its nomenclature, and the integration strategy, can be found in previous publications,^{8,9} including a discussion of the main results. The ion and electron equations are presented here in abridged form for convenience:

$$\nabla \cdot (n\mathbf{u}_i) = 0, \quad (1)$$

$$m_i (\mathbf{u}_i \cdot \nabla) \mathbf{u}_i = e (-\nabla\phi + \mathbf{u}_i \times \mathbf{B}), \quad (2)$$

$$0 = -T_e \nabla \ln n - e (-\nabla\phi + \mathbf{u}_e \times \mathbf{B}). \quad (3)$$

The main characteristics of the model stem from the hypotheses of: (1) negligible collisions, i.e. that the Hall parameter $\chi_H = eB/m_e\nu_e \gg 1$; and (2) completely magnetized electrons and negligible electron inertia, i.e. electron Larmor radius $\ell_e = \sqrt{m_e T_e}/(eB) \ll R$, with R the macroscopic length of the plasma. Electron streamtubes are therefore assumed to coincide with magnetic streamtubes. Ions, however, are only partially magnetized, and separate inwards from the electron streamtubes depending on their magnetization degree, giving rise to longitudinal currents⁸ and facilitating detachment.¹³ The validity of these assumptions is justified inasmuch as an efficient MN requires that at least the electrons are magnetized, so that the plasma will describe the geometry of the magnetic field, and that the flow collisionality is low to achieve good magnetic confinement. The resultant model is dependent on the geometry and intensity of the magnetic field (the latter measured by the non-dimensional ion gyrofrequency, $\hat{\Omega}_{i0} = eBR/\sqrt{m_i T_e}$, which is the key parameter that controls ion magnetization), and the initial conditions at the nozzle throat.

For a given magnetic field \mathbf{B} , Eqs. (1)–(3) are hyperbolic if ions are supersonic, and they can be integrated with the method of characteristics (MoC). This leads to a highly accurate and computationally inexpensive integration scheme.¹⁴ As a consequence, DIMAGNO is regarded as a valuable tool for validation of more complex codes such as HPMN.

As pointed out in the introduction, DIMAGNO reproduces the fundamental MN physics of plasma expansion and acceleration, electric currents, thrust generation, etc., and has been used to study the main aspects of the operation of these devices. Certain advanced physics can also be analyzed by extending this model. For instance, the plasma-induced magnetic field, which can play an important role in detachment, can be taken into account with a simple iteration procedure.¹⁵ The influence of collisions was recently studied

with a perturbation analysis.^{9,16} The dominant electron inertia effects (finite Larmor radius effects) can be easily incorporated into the model.^{17,18} Support for multiple-temperature electron distributions has been added, allowing the study of the formation of quasi-double-layers in the flow.¹⁹ Latest developments include the capability to simulate the flow beyond the magnetic turning point to analyze the far-field plume.¹³

III. Hybrid PIC/fluid model (HPMN)

The core of the hybrid model used here inherits from the well-known HPHall2 hybrid code,¹² an improved version of HPHall,²⁰ which was designed to describe the plasma physics in a Hall thruster. The fundamentals and intricacies of the new HPMN code were presented in Ref. 11.

Heavy species (neutrals and ions) are treated as macroparticles in a conventional PIC subcode. The spatial grid is axisymmetric and structured. Collisions that involve ions and neutrals can be accounted for using Monte-Carlo methods. Main properties of the quasineutral plasma provided by the PIC subcode are the plasma density and ion currents.

HPMN models electrons as a magnetized fluid. Main differences compared with DIMAGNO are (1) the inclusion of collisions in the momentum equation and (2) the possibility of taking into account ionization processes. Thus, Eqs. (1) and (3) of previous section are extended here to include these terms,

$$\begin{aligned}\nabla \cdot (n\mathbf{u}_i) &= \nabla \cdot (n\mathbf{u}_e) = \dot{n}_e \quad (\Rightarrow \nabla \cdot \mathbf{j} = 0), \\ 0 &= -T_e \nabla \ln n - e(-\nabla\phi + \mathbf{u}_e \times \mathbf{B}) + m_e \nu_e \mathbf{u}_e.\end{aligned}\tag{4}$$

The fluid model of electrons is based on projecting Eqs. (4) and (5) onto the magnetic reference frame, $\mathbf{1}_{\parallel}, \{\mathbf{1}_{\perp}, \mathbf{1}_{\theta}\}$, where, $\mathbf{1}_{\parallel} = \mathbf{B}/B$, and $\mathbf{1}_{\perp} = \mathbf{1}_{\theta} \times \mathbf{1}_{\parallel}$ is the normal unit vector to the magnetic field. The result of splitting Eq. (5) along each of these directions is, respectively,

$$e\phi(r, z) = -H_e(\psi) + T_e(\psi) \ln n(r, z),\tag{6}$$

$$u_{\theta e} = -\chi_H u_{\perp e},\tag{7}$$

$$u_{\perp e} = -\frac{r\chi_H}{1 + \chi_H^2} \frac{\partial H_e}{\partial \psi},\tag{8}$$

where only azimuthal resistivity has been kept due to its zero-order character on the definition of $u_{\perp e}$, ψ is the magnetic streamfunction, and the rest of symbols are conventional

Equation (6) constitutes the Boltzmann relation in the parallel direction, in which $-H_e/e$ is the thermalized potential, known from flow conditions at the MN throat. Equations (7) and (8) describe, respectively, the azimuthal and perpendicular behaviour of the electron flow. Notice that the last one becomes $u_{\perp e} = 0$ in the collisionless limit $\chi_H \rightarrow \infty$, recovering the corresponding expression of DIMAGNO. Eq. (8) may be regarded as the Ohm's law in the perpendicular direction.

Local current ambipolarity (LCA) is not fulfilled everywhere within the plasma domain, even for a globally current-free plume.⁸ This idea stands out from Eq. (4) when it is projected along $\mathbf{1}_{\perp}$ and integrated on each magnetic tube:

$$\frac{\partial I_{\perp}(\psi)}{\partial \psi} = \frac{2\pi j_z}{B \cos \alpha} \Big|_{throat} - \frac{2\pi j_z}{B \cos \alpha} \Big|_{end},\tag{9}$$

where $I_{\perp}(\psi) = I_{\perp i} + I_{\perp e}$ is the net current across the magnetic surface given by $\psi = \text{const}$, between the throat ($z = 0$) and downstream end sections ($z = z_{end}$), in the direction of $\mathbf{1}_{\perp}$. Ion current $I_{\perp i}$ is provided by the PIC sub-code, whereas electron $I_{\perp e}$ stems from Eq. (8) and the local density n (resulting from PIC calculations). Both of them ($j = i, e$) can be expressed as

$$I_{\perp j} = q_j \int_{\psi} n u_{\perp j} d\sigma,\tag{10}$$

with $d\sigma$ a differential area element of the magnetic surface.

Electrons are treated as an isothermal species in this model. We emphasize that a non-isothermal model $T_e(\psi)$ could be easily considered once a closure for the heat flux is provided for the energy equation. In order to facilitate the comparison of the results with DIMAGNO, ionization mechanisms are also switched off.

IV. Upstream Plasma characterization

The focus of this work is on the MN flow of plasmas generated using a helicon plasma source. In this section the fluid model of helicon source described in Ref. 21 is used to obtain the radial equilibrium and plasma fluxes at the throat. This boundary condition serves then as the starting point of integration for the two codes described above.

Within the dielectric tube, radial plasma pressure is balanced by (1) the force created by the external axial magnetic field and plasma azimuthal currents, and (2) the radial ambipolar electric field. The same electric field pulls ions towards the wall of the source. The higher the magnetic field, the stronger the magnetic confinement compared to the electric one, and the smaller the plasma losses to the wall.

The plasma is accelerated along the source up to the ion sonic velocity, $c_s = \sqrt{T_e/m_i}$, reached at the exit section, where the MN throat is located.

The matching between source and MN requires some additional comments. In the case of DIMAGNO, the profile requires some adaptation as follows: first, due to the requirement of hyperbolicity of the equations, the initial Mach number is chosen $M_0 = 1.01$, slightly higher than 1. This introduces a small error ($< 5\%$) in continuity, momentum and energy conservation equations. (2) DIMAGNO's collisionless plasma flow must be parallel to \mathbf{B} at the plasma edge. This is dealt with by cutting off a small fraction of the plasma flow near the edge, where the largest radial velocity is located. Since density is low in this region, the amount of plasma which is disregarded in the nozzle simulation of DIMAGNO is negligible. The small radial velocity within the retained plasma is also neglected.

In the matching with the HPMN model, on the other hand, we need to express the plasma flux using a kinetic formulation, because ions are modeled by a PIC code. These particles are injected through the MN throat along the \mathbf{B} direction according to a distribution function of particles velocity. This function must retain plasma properties at the source exit section (i.e. density n and plasma flux $n\mathbf{u}$).

IV.A. MN throat conditions

The chosen source parameters are listed next: ion mass $6.6 \cdot 10^{-26}$ kg (Ar), mass flow $\dot{m} = 0.1$ mg/s, tube radius $R = 0.01$ m and length $L = 0.1$ m, plasma temperature $T_e = 10$ eV, and magnetic field intensity $B_0 = 200$ G (assumed constant along the dielectric tube).

For these values, the non-dimensional ion gyrofrequency is $\hat{\Omega}_{i0} = ReB/\sqrt{m_i T_e} \simeq 0.1$. The useful power, in accordance with enumerated parameters, is in the power range 50–100 W, so this study refers to the analysis of a mini-helicon plasma thruster (e.g. Ref. 4).

Figure 1a shows the radial structure of the plasma density. Plasma radial velocity is depicted in 1b. Taking into account that $-e\phi \sim 1/2 m_i u_{ri}^2$, the radial electric field can be neglected, except at the vicinity of the plasma edge (inertial layer, which precedes the Debye sheath. Ref. 22).

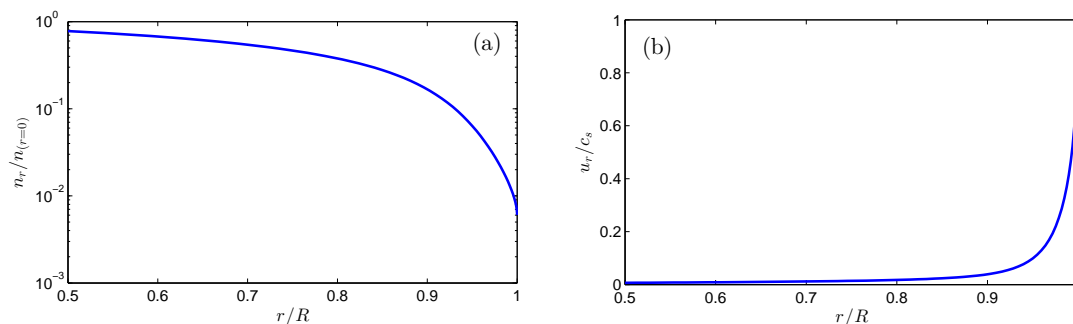


Figure 1. (a) Plasma density at the MN throat $n(r)/n_{r=0}$. (b) Plasma radial velocity u_{ri}/c_s .

Simulations of the source indicate that propellant utilization η_u , which relates ion flow at the source exit to the total mass flow, is over 92%. Consequently, the flux through MN throat is practically fully-ionized, and residual neutral density is low enough to neglect plasma ionization within the plasma plume. Increasing the magnetic field up to 600 G, η_u goes up to $\simeq 99\%$.

V. Comparison of results

Figure 2 presents 2D maps of the plasma density in the MN plume for both codes. HPMN reproduces the same behaviour of DIMAGNO, and the agreement in this regard is high. Numeric results obtained using the hybrid model also fit with the full fluid code response. Spatial gradients of the plasma density in HPMN are coherent with DIMAGNO. The large radial rarefaction is reproduced by both hybrid and fluid codes. Obviously, DIMAGNO is still more accurate because of its MoC approach.

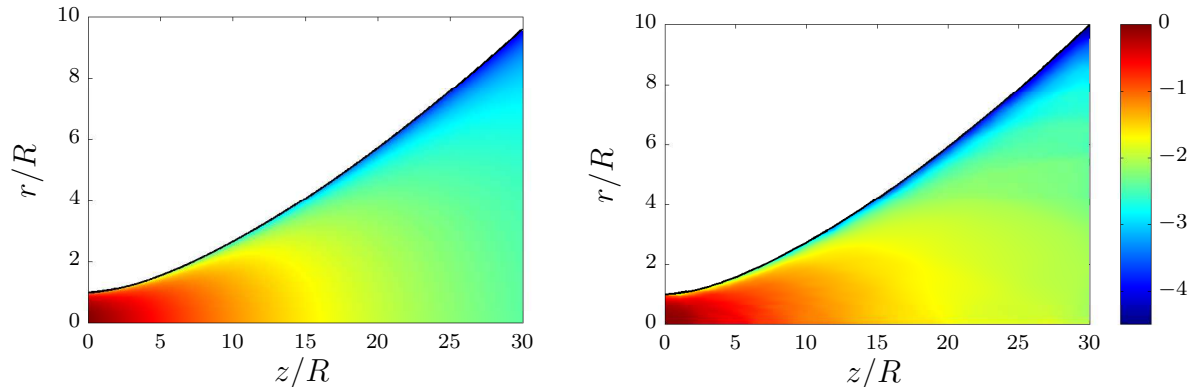


Figure 2. Plasma density $\log_{10} n_e$ (part/m^3) DIMAGNO (left) and HPMN (right).

The correlation between plasma density maps allows to know beforehand that electric potential, Figure 3, should exhibit similar results. According to Eq. (6), electric potential ϕ is equivalent to the thermalized potential, which is constant along each magnetic surface, plus a correction comparable to the plasma temperature and $\ln n$. The thermalized potential is the same in both models because it only depends on MN throat conditions. Consequently, electric potential from HPMN agrees with DIMAGNO results. However, a slight mismatch on the results is appreciable. These local deviations appear as a consequence of PIC fluctuations in properties and interpolation errors. Consequently, equipotential surfaces obtained with the hybrid model are not as smoothly defined as in DIMAGNO.

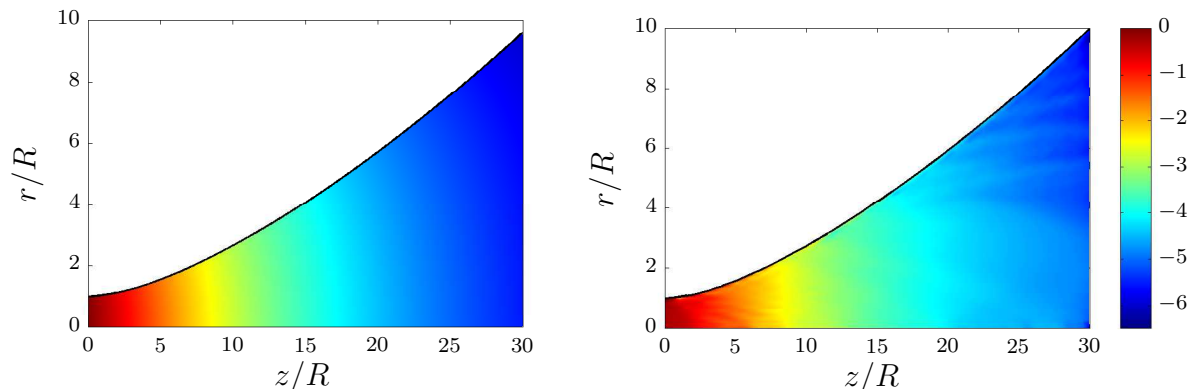


Figure 3. Electric potential $\phi(V)$ DIMAGNO (left) and HPMN (Right).

This is further manifested by the potential drop along the axis line, relative to the potential at the MN throat, is about $5.5T_e$ at $z = 0.3$ m as shown in Figure 4. The tendency in both models is almost the same from the MN throat until $z = 0.1$ m. However, the loss of correlation from $z = 0.1$ m and downstream along the plasma plume cannot be neglected. The numerical behaviour of HPMN downstream, where MN area is by far larger than that measured at the throat section, requires some comments.

First, in spite of injecting a huge number of macroparticles per cell (N) at the MN throat, it is not possible to avoid the low N we find at the far plume. This reduction is due to the strong rarefaction that takes place in the plume, plus the lack of ionization processes that would increase N .

Second, the reduction of N induces the statistical failure of the weighting algorithms as shown in Figure

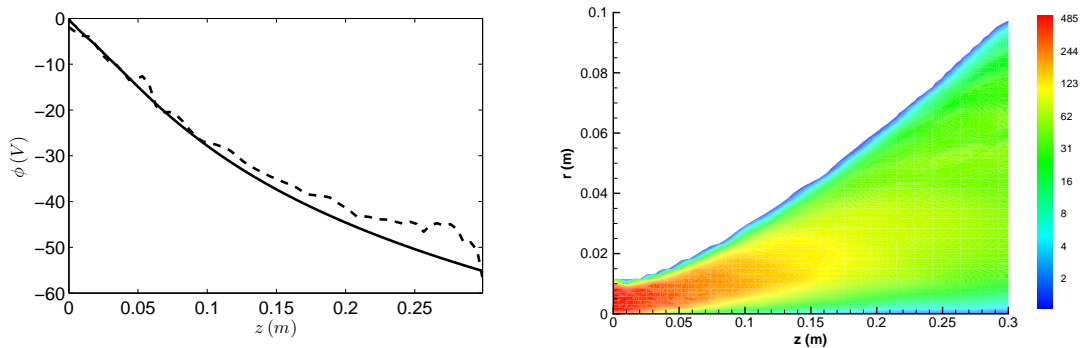


Figure 4. Left: Electric potential along axis, DIMAGNO (solid line) and HPMN (dashed line). Right: Number of particles per cell, N , according to HPMN simulation.

5 (right), which plots the ion Mach number distribution within the plasma plume $M_i(z, r) = \sqrt{u_{zi}^2 + u_{ri}^2}/c_s$. The natural response to the monotonically drop of the electric potential ϕ (Figure 3) should be a continuous acceleration of charged particles, as depicted in DIMAGNO results, Figure 5 (left). In fact, all ions in the PIC simulation are (independently) accelerated along z positive direction. But the macroscopic flow velocity \mathbf{u} obtained from weighting across particles does not retain this behaviour because it is influenced by the low N , the particle velocity dispersion, and the numerical density background, n_{bg} .

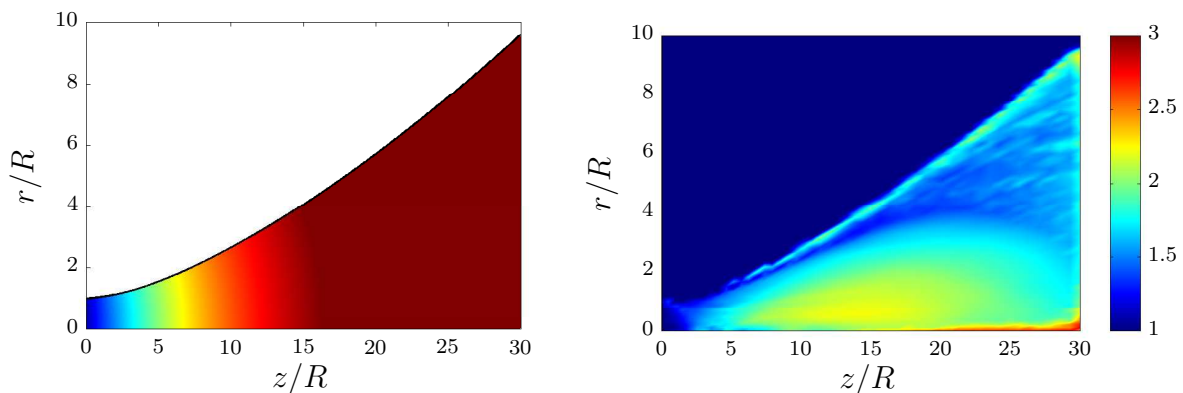


Figure 5. Ion Mach number M_i , DIMAGNO (left), and HPMN (right).

This background is necessary to avoid PIC model inconsistencies. Nonetheless, here is still overly large and produces an undesirable effect. In this research, the treatment of n_{bg} has been improved compared with the model in Ref.¹¹ Now, n_{bg} is reduced progressively to a more appropriate value according to the average value of N .

This upgrade is not enough to correct or improve the weighting algorithm results that try to reproduce the second or higher-order moments of the ion distribution function, i.e., particle flux $n\mathbf{u}$, momentum flux and successive moments. The first-order moment of the ion distribution function, necessary to deal with the ion density (i.e. the plasma density), is not affected by the particle velocity dispersion, and has been improved thanks to the new model.

Plasma density governs the effective electron collision frequency, $\nu_e = \nu_{ei} = n_e R_{ei}$, which drives the electron perpendicular dynamics inside the plasma plume. R_{ei} is the rate of *electron-ion* collisions which depends on the plasma temperature and the Coulomb logarithm. In fact, the diffusive electron transport in the plasma plume is controlled by the Hall parameter χ_H , which is illustrated in Figure 6 (left). Perpendicular currents, Eq. (10), are depicted in Figure 6 (right). All currents are zero at the axis of symmetry. I_e increases radially due to collisions, which permit electrons to move outward (see Eq. (8)), but near the plasma edge it decreases again due to the significant growth of χ_H . Magnetic field intensity increases there, and collisions decrease at the same rate as the density drop.

Results from HPMN support the collisionless limit of DIMAGNO as a good approximation for large values of χ_H . Both models present a similar response of $u_{\theta e}$ (Figure 7) as expected, since collisions do not

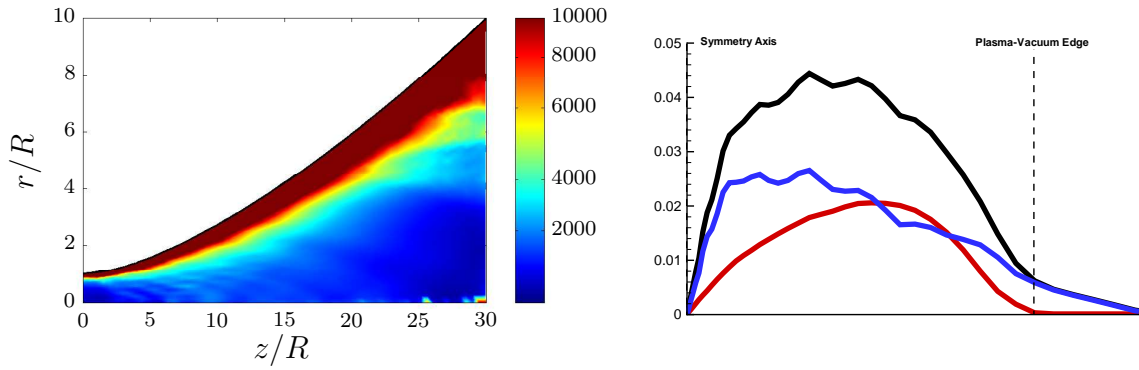


Figure 6. Left: Hall parameter χ_H in the HPMN simulation. Right: Inward-pointing perpendicular electric currents (Amperes) through magnetic surfaces between axis line and plasma edge surface, both limits are indicated by vertical dashed-lines (HPMN). Total current I_{\perp} in black, ion current I_i in blue, electron current I_e in red. The ion current at the Helicon source exit section, using the values presented in section IV.A, is $0.23A$.

affect $u_{\theta e}$ up to first order. This property varies according to Eq. (7), which in the DIMAGNO limit only depends on the thermalized potential and the MN divergence.

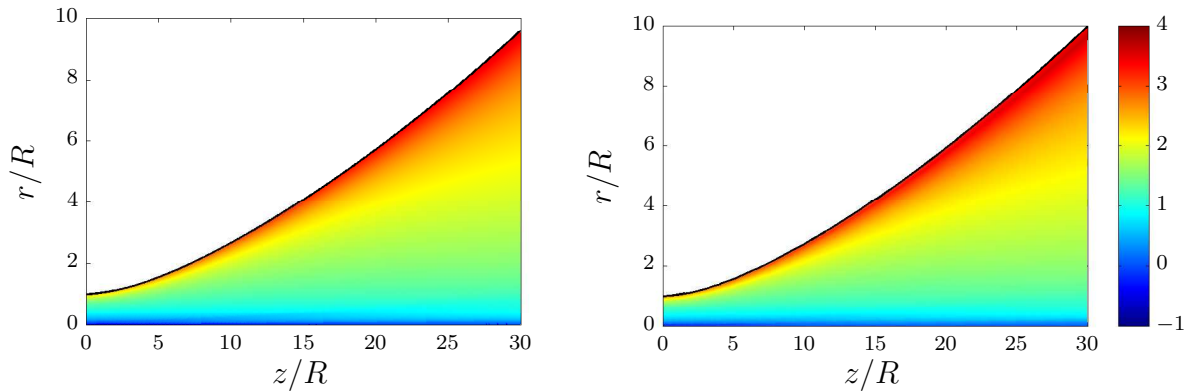


Figure 7. Electrons azimuthal velocity $\log_{10}(u_{\theta e})$. DIMAGNO (left), and HPMN (right).

Improvements on HPMN, such as n_{bg} progressive reduction, have allowed a fine closure of I_e at the vicinity of the plasma edge, Eq. (10), which was one of the difficulties encountered in the previous version. Near the plasma edge, large gradients of some plasma properties cannot be captured by the PIC mesh, producing high electric fields that disturb the behaviour of the PIC subcode. To deal with this problem a finer PIC submesh will be required in future work, to assess the gentle plasma-vacuum edge, increasing by far, the computational effort. The coarse grid of the PIC subcode near this region and its interaction with the magnetic frame (electron subcode), using interpolation algorithms, also explain the unexpected closures and mismatch of the perpendicular currents.

The global error committed at the MN (HPMN model) can be estimated in terms of the charge conservation law, Eq. (4). This error is lower than 5% for electrons. For ions it is lower than 10% and can be neglected if ion charge balance is carried out on the full domain. This higher error is attributable to the interpolation error between the PIC mesh and the magnetic grid at the plasma edge.

Finally, it is interesting to compare the thrust gain due to the MN. Dimensionless thrust of both models is depicted in Figure 8, using the ion momentum plus plasma pressure at the source exit, F_0 , as the reference value. The monotonic HPMN thrust increase correlates very well with the thrust gain obtained by DIMAGNO. The last one includes the contribution of ion momentum flux and plasma pressure, while the thrust computed by HPMN only takes into account the ion momentum flux that flows through each $z = \text{const}$ surface. Despite this difference, HPMN thrust gain is higher than DIMAGNO's. Note that a lower thrust would be expected in the HPMN results because it neglects the plasma pressure contribution. Probably, this variation is due to the fluid-kinetic conversion of the ion flow injected at the MN throat, which might introduce a slight error on plasma momentum conservation law.

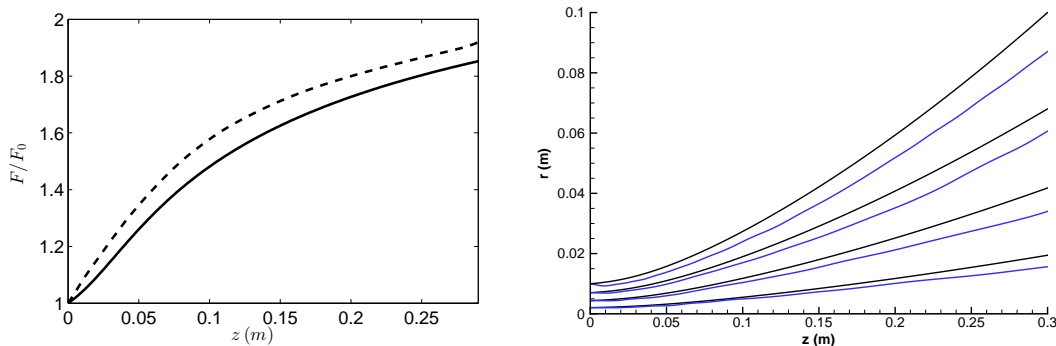


Figure 8. Left: MN dimensionless thrust gain F/F_0 as a function of the MN length z . F_0 is the ion momentum plus the plasma pressure at the source exit section (MN throat). Right: Ion detachment, black solid lines depicts the magnetic stream surfaces, and blue lines show ions streamlines.

Ion detachment is depicted in Figure 8 (right). Ion streamlines, obtained in accordance with the ion current density, clearly detach inwards from the magnetic surfaces. Overall, this result agrees with DIMAGNO, Refs.^{8,13} This behaviour also explains the increasing ion current through magnetic surfaces $I_i > 0$ (Figure 6 right). Near the vacuum edge, where density is lower, ion streamlines should move closer to magnetic surfaces to fulfil the quasineutral-plasma hypothesis.

VI. Conclusion

A comparison between DIMAGNO and HPMN codes, which describe the plasma flow in a magnetic nozzle, has been carried out in terms of main plasma properties, with the aim to validate the later and correlate results.

The cleanliness and high resolution of DIMAGNO, inherent to the fluid model and method of characteristics, is unattainable with the hybrid code. Despite this disadvantage, some HPMN results, such as plasma density, electric potential or electron azimuthal velocity, agree very well with fluid model results. Even the thrust gain computed by HPMN correlates closely with DIMAGNO.

The central advantage of HPMN is that it introduces collisions in the nozzle flow, and thus allows to study phenomena not available in DIMAGNO.

Regarding perpendicular diffusion and according to the case simulated here (parameters of Sec. IV), HPMN measures a low electron conductivity across magnetic surfaces. This result supports again the DIMAGNO hypothesis of collisionless plasma.

This work also points out some limitations of HPMN to be overcome in the future. First, the failure of weighting algorithms if the number of particles-per-cell drops as a consequence of the diverging geometry. Second, the response of the PIC subcode is slightly perturbed near the plasma-vacuum edge due to the coarse mesh of the PIC subcode. In this regard, the grid should be refined in order to improve overall accuracy.

Acknowledgments

This work has been sponsored by the Air Force Office of Scientific Research, Air Force Material Command, USAF, under grant number FA8655-12-1-2043. The U.S Government is authorized to reproduce and distribute reprints for Governmental purpose notwithstanding any copyright notation hereon. Additional support comes from the Spanish Government (Project AYA-2010-61699).

References

- ¹Ziamba, T., Carscadden, J., Slough, J., Prager, J., and Winglee, R., "High Power Helicon Thruster," *41th AIAA/ASME/SAE/ASEE Joint Propulsion Conference & Exhibit*, AIAA 2005-4119, 2005.
- ²Batishchev, O., "Minihelicon Plasma Thruster," *IEEE Transaction on Plasma Science*, Vol. 37, 2009, pp. 1563–1571.
- ³Charles, C., Boswell, R., and Lieberman, M., "Xenon ion beam characterization in a helicon double layer thruster," *Applied Physics Letters*, Vol. 89, 2006, pp. 261503.
- ⁴Pavarin, D., Ferri, F., Manente, M., Curreli, D., Guclu, Y., Melazzi, D., Rondini, D., Suman, S., Carlsson, J., Bramanti,

C., Ahedo, E., Lancellotti, V., Katsonis, K., and Markelov, G., "Design of 50W Helicon Plasma Thruster," *31th International Electric Propulsion Conference*, IEPC 2009-205, 2009.

⁵Krülle, G., Auweter-Kurtz, M., and Sasoh, A., "Technology and application aspects of applied field magnetoplasmadynamic propulsion," *J. Propulsion and Power*, Vol. 14, 1998, pp. 754–763.

⁶Tikhonov, V., Semenikhin, S., Brophy, J., and Polk, J., "Performance of 130kw mpd thruster with an external magnetic field and Li as a propellant," *Proceedings of the 25 th International Electric Propulsion Conference*, 1997, pp. 728–733.

⁷Diaz, F., Squire, J., Bengtson, R., Breizman, B., Baity, F., and Carter, M., "The Physics and Engineering of the VASIMR Engine," *36th AIAA/ASME/SAE/ASEE Joint Propulsion Conference & Exhibit*, AIAA 2000-3756, 2000.

⁸Ahedo, E. and Merino, M., "Two-dimensional supersonic plasma acceleration in a magnetic nozzle," *Physics of Plasmas*, Vol. 17, 2010, pp. 073501.

⁹Ahedo, E. and Merino, M., "On plasma detachment in propulsive magnetic nozzles," *Physics of Plasmas*, Vol. 18, 2011, pp. 053504.

¹⁰Merino, M. and Ahedo, E., "Simulation of plasma flows in divergent magnetic nozzles," *IEEE Transactions on Plasma Science*, Vol. 39, No. 11, 2011, pp. 2938–2939.

¹¹Navarro, J. and Ahedo, E., "Hybrid model simulation of a plasma plume in a magnetic nozzle," *32th International Electric Propulsion Conference, Wiesbaden, Germany*, IEPC 2011-048, 2011.

¹²Parra, F., Ahedo, E., Fife, M., and Martínez-Sánchez, M., "A two-dimensional hybrid model of the Hall thruster discharge," *Journal of Applied Physics*, Vol. 100, 2006, pp. 023304.

¹³Merino, M. and Ahedo, E., "Magnetic Nozzle Far-Field Simulation," *48th AIAA/ASME/SAE/ASEE Joint Propulsion Conference & Exhibit*, No. AIAA-2012-3843, AIAA, Washington DC, 2012.

¹⁴Zucrow, M. and Hoffman, J., *Gas dynamics*, Wiley, New York, 1976.

¹⁵Merino, M. and Ahedo, E., "Plasma detachment mechanisms in a magnetic nozzle," *47th AIAA/ASME/SAE/ASEE Joint Propulsion Conference & Exhibit*, No. AIAA-2011-5999, AIAA, Washington DC, 2011.

¹⁶Ahedo, E. and Merino, M., "Preliminary assessment of detachment in a plasma thruster magnetic nozzle," *46th AIAA/ASME/SAE/ASEE Joint Propulsion Conference & Exhibit*, No. AIAA 2010-6613, AIAA, Washington DC, 2010.

¹⁷Ahedo, E. and Merino, M., "On electron inertia and current ambipolarity in magnetic nozzles models," *32th International Electric Propulsion Conference, Wiesbaden, Germany*, edited by F. Electric Rocket Propulsion Society, IEPC 2011-050, 2011.

¹⁸Ahedo, E. and Merino, M., "Two-dimensional plasma expansion in a magnetic nozzle: separation due to electron inertia," *Physics of Plasmas*, Vol. 19, 2012, pp. 083501.

¹⁹Merino, M., "2D plasma flow in a magnetic nozzle with a bi-modal Electron Energy Distribution Function," *50th AIAA Aerospace Sciences Meeting*, No. AIAA 2012-0139, AIAA, Washington DC, 2011.

²⁰Fife, J., *Hybrid-PIC Modeling and Electrostatic Probe Survey of Hall Thrusters*, Ph.D. thesis, 1998.

²¹Navarro, J., Merino, M., and Ahedo, E., "A fluiddynamic performance model of a helicon thruster," *48th AIAA/ASME/SAE/ASEE Joint Propulsion Conference & Exhibit*, No. AIAA-2012-3955, AIAA, Washington DC, 2012.

²²Ahedo, E., "Parametric analysis of a magnetized cylindrical plasma," *Physics of Plasmas*, Vol. 16, 2009, pp. 113503.